Table II: Ion-clamped static macroscopic dielectric constants ε_∞ calculated using density functional perturbation theory and PAW method for various $k-$point sets: Γ indicates a grid centered at Γ, whereas Monkhorst-Pack (MP) grids do not include the Γ point. values for $\varepsilon_{\rm mic}^{\rm LR}$ neglect the local field effects, and are obtained using linear response theory. $\varepsilon^{\rm cond}$ are values obtained by summation over conduction band states.

Na-hp4	N_k (IBZ)	$\varepsilon_{\rm mic}^{\rm LR}$	$\varepsilon^{\rm cond}$	$\varepsilon_{\rm mic}^{\rm LR}$	$\varepsilon^{\rm cond}$
		E$\|\|$**x** (**y**)		**E**$\|\|$**z**	
$(18\times18\times12)\,\Gamma$	637	5.785	5.457	11.116	10.761
$(21\times21\times14)\,\Gamma$	968	5.785	5.458	11.055	10.701
$(24\times24\times16)\,\Gamma$	1413	5.786	5.458	11.028	10.674
$(18\times18\times12)$ MP	1512	5.786	5.459	10.900	10.546

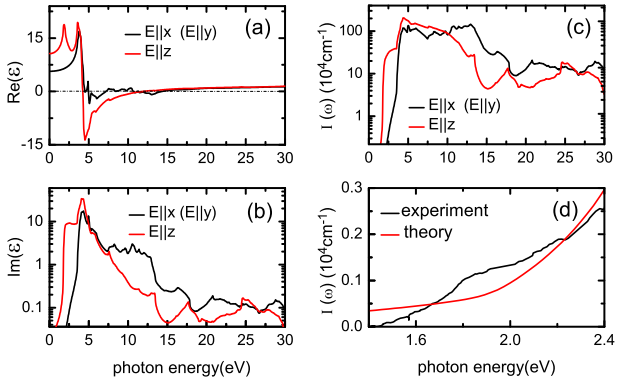

Figure 5: (Color online) (a) Real part and (b) imaginary part of the dielectric function, and (c) absorption spectrum $I(\omega)$ along the principle axes at 320 GPa. (d) Absorption spectrum $I(\omega)$ in the energy range from 1.4 eV to 2.4 eV at 200 GPa. In (d) the red line is theoretical value, while the black line represents the experimental data reported in Ref. [8].

dielectric constants with good convergence within 0.001 for **E**$\|\|$**x** (**y**) and 0.09 for **E**$\|\|$**z**. The value of $\varepsilon_{\rm mic}^{\rm LR}$ can be compared with experimental data. Obviously, ε_∞ is 5.785 and 11.028 in **E**$\|\|$**x** (**y**) and **E**$\|\|$**z** directions, respectively. The obtained values can be as important reference for further experimental measurements of Na-hp4.

Our calculated optical spectra cover the photon energy range of 30 eV. In order to show the details clearly, we use logarithm longitudinal scale for the imaginary part of dielectric constant Im (ε) and absorption coefficient $I(\omega)$. Im (ε) shows mainly five peaks both in **E**$\|\|$**z** direction and in **E**$\|\|$**x** (**y**) directions. In **E**$\|\|$**z** direction, these peaks correspond to the photon energy of 2.54, 4.31, 13.37, 17.7 and 24.64 eV, while in **E**$\|\|$**x** (**y**) directions, 4.31, 10.54, 16.34, 20.8 and 28.8 eV, respectively. The peak at 2.54 eV originates from the transition from $3p$ to $3d$ corresponding to the topmost valence band to bottommost conduction band, while the peak at 4.31 eV is attributed to the transition from $3s$ to $3p$. At 4.31 eV and 13.37 eV in **E**$\|\|$**z** direction and 4.31 eV and 16.34 eV in **E**$\|\|$**x** (**y**) directions, the sign of Re (ε) changes, which predict the anisotropy of the polarized Re (ε) spectra. In the range around 13.37 eV and 16.34 eV, Im $(\varepsilon)$is very low and thus the conditions for a plasma resonance are satisfied[21]. Hence, there are strong resonance maxima at these energies in the calculated energy-loss spectra $L(\omega)$ for these polarizations, as can be seen from Fig. 6(c). The other seven high-energy peaks can all be attributed to transitions from the top two valence bands to the upper conduction bands, without deep-lying valence orbitals participating in the interband transitions. These also explain the origin of the peak structure in the absorption coefficient $I(\omega)$ and reflectivity $R(\omega)$ spectra. The absorption spectra remains nearly zero in the visible photon energy, which implies that Na-hp4 is transparent to visible light. As seen from Fig. 5(c), Na-hp4 remains transparent to light with higher frequency in **E**$\|\|$**x** (**y**) direction than in **E**$\|\|$**z** direction. In Fig. 5(d), we present $I(\omega)$ in the photon energy range from 1.4 eV to 2.4 eV at 200 GPa along with the previously reported experimental measurement[8]. Here we assume the sample thickness is 8 μm. As all know, the band gap can be deduced by extrapolating the absorption to zero. It is concluded that the results from theoretical calculation and experiment agree well except that the theoretically predicted band gap is smaller than the experiment, the origin of which is the local-density approximation. In addition, it should be noted that the present calculation only pertains to the electronic response, and does not include the effects of lattice vibrations that dominate the experimental absorption spectrum in the low frequency region. Thus we can not derive the complete agreement with experimental results.

In Fig. 6, we show the main optical spectra including optical conductivity, reflective spectrum, energy-loss spectrum, extinction and refractive indices in a photon energy width of 30 eV. The peak of optical conductivity in **z** direction is almost twice as large as that in **x** and **y** directions. The reflectivity spectrum is distinct from the drude-type spectrum, which means Na-hp4 is no longer metallic. The reflectivity is small at visible optical energy, which ensures the transparency of Na-hp4. During the range about 5 eV to 10 eV, the reflective index remains almost constant as 60% in **E**$\|\|$**z** direction and 20% in **E**$\|\|$**x** (**y**) direction. Refractive indices of a crystal are closely related to electronic polarizability of ions and the local field inside the crystal. Another interesting point connected with the refractive indices is the electro-optic effect. We present the refractive indices $n(\omega)$ in Fig. 6(d). The low-frequency refractive index along **E**$\|\|$**x** (**y**) and **E**$\|\|$**z** direction are calculated as $n_{x(y)} = 2.38$ and $n_z = 3.26$ respectively. It is clear that the light polarized parallel to the **z** axis is more refracted than that with polarization along the **x** and **y** axes. This indicates the